Influence of the demagnetization on the polarization of the thermal radiation emitted by hot cobalt wires

A. F. Borghesani[a,b,*], M. Guarise[c,1], G. Carugno[b]

[a] *CNISM Unit, Department of Physics and Astronomy, University of Padua, Italy*
[b] *Istituto Nazionale Fisica Nucleare, sez. Padova, Italy*
[c] *Department of Physics and Astronomy, University of Padua, Italy*

Abstract

The polarization P of thermal radiation emitted by a hot cobalt wire in the temperature range from $T \approx 400\,\mathrm{K}$ up to melting is studied for the first time. The radiation is linearly polarized perpendicularly to the wire. P decreases from 30 % just above room temperature down to 6.5 % near melting and is continuous across the martensitic *hcp*−*fcc* transition at $T_m \approx 700\,\mathrm{K}$ and across the Curie point at $T_c \approx 1400\,\mathrm{K}$. However, P shows a rapid decrease for $T \gtrsim 1000\,\mathrm{K}$ and, contrary to previous measurements with tungsten wires, it hysteretically behaves if the temperature change is reversed. This behavior is rationalized by accounting for the thermal demagnetization of the wire with magnetic domain size change.

Keywords: cobalt wire, thermal radiation, linear polarization, demagnetization, hysteresis.

1. Introduction

The dynamics of the domain structure of magnetic materials has long attracted a great deal of interest and is presently a field of intense research. The domain wall (DW) motion is thoroughly investigated for its relevance in fundamental science and applications. Thermally activated [1], magnetic field [2]

*Corresponding author
Email address: armandofrancesco.borghesani@unipd.it (A. F. Borghesani)
[1] Present address: Dipartimento di Fisica e Scienze della Terra, University of Ferrara, and Istituto Nazionale di Fisica Nucleare, Sezione di Ferrara, Ferrara, Italy

and/or current [3] driven DW creep and flow, DW depinning [4, 5] or precessional modes [6], thermally driven diffusive DW motion [7], thermally- or field driven domain reversal [8–10], magnetic viscosity [11, 12], among many other topics, are studied with a number of techniques in several samples of different composition, size, and geometry because of their relevance in many technological applications, e.g., for spintronics [13], for magnetic recordings [14], and for new sensors [15], also including geophysics and paleomagnetism [16, 17].

The coupling of radiation with the sample properties is exploited to investigate its domain structure and dynamics via the magnetooptical Kerr effect (MOKE) [18–20]. As it is based on the rotation of the polarization plane and intensity change of visible light reflected off a magnetic material, MOKE is limited to provide pieces of information on the material surface. For instance, the surface domain structure, magnetization switching and reversal in amorphous microwires under different experimental conditions have been succesfully studied by MOKE techniques [21–24]. Additionally, it is known that there exists another magneto-optical effect, which leads to the magnetically induced depolarization of electromagnetic waves scattered off a plasma [25].

However, pieces of information on the bulk properties and structure of a sample can also be gathered by investigating the properties of the thermal radiation emitted by a thin metallic wire. Actually, a hot body at temperature T and of size larger than the typical thermal wavelength $\lambda_T = hc/k_{\rm B}T$, where h is the Planck's constant, c is the speed of light, and $k_{\rm B}$ is the Boltzmann constant, emits incoherent and unpolarized radiation. Nonetheless, if the phase space available for the collective fluctuations of the electron gas is reduced by geometrically limiting the radiator size, the thermal radiation acquires a degree of linear polarization [26]. This fact is important because in recent years there is an interest to produce nano-heaters and nano-light sources for engineering and physics applications [27–29]. Recently, we have carried out measurements of the linear polarization P of the radiation emitted by hot tungsten wires. We have found that it is partially polarized perpendicular to the symmetry axis of the wire because the thermally driven collective transverse fluctuations of the

electron sea are limited by the wire boundaries and that its polarization degree decreases from $P \approx 30\,\%$ for $T \approx 500\,\mathrm{K}$ down to $\approx 15\,\%$ just before melting at $T \approx 3700\,\mathrm{K}$. We have shown that the experimental behavior of P is reproduced by computing the absorption efficiency of radiation impinging on a cylindrical object of known radius and that it is intimately related to the bulk optical properties of the material [30].

Therefore, we have decided to investigate the polarization of the thermal radiation emitted by a thin cobalt wire in order to see if pieces of information on structure and thermally driven dynamics of the magnetic domains of the material can be obtained from optical measurements on a macroscopic sample.

Cobalt is primarily chosen because of its interesting magnetic and crystalline properties. Its ferromagnetic-paramagnetic transition occurs at a Curie temperature of $T_c \approx 1400\,\mathrm{K}$. Moreover, it shows a martensitic transition at $T_m \approx 700\,\mathrm{K}$ from the low-T *hcp*- to the high-T *fcc* structure. At low temperature the hexagonal axis is the direction of easiest magnetization, whereas in the *fcc* phase at high temperature the metal becomes isotropic [31]. As the present experiment is carried out as a function of T up to melting, cobalt offers a unique opportunity to investigate a rich realm of behaviors.

The present experiment, as it is carried out even at high temperature including the Curie temperature of the sample, might provide helpful knowledge for studies in the field of heat-assisted magnetic recording [32].

2. Experimental Details

The apparatus and the technique are the same used for investigating the polarization of the thermal radiation emitted by tungsten wires and are thoroughly described in literature [30]. We recall here the main features of the experiment. A 7 mm long cobalt wire of radius $R_0 = 50\,\mu\mathrm{m}$ (99.99 %+ purity, Goodfellow Cambridge Ltd) is mounted in a nonmagnetic vacuum cell. The wire is heated by an adjustable d.c. bias current that sets its temperature, which is linear in the d.c. dissipation.

The determination of the wire temperature follows the procedure outlined in our previous paper on tungsten [30]. The energy transport equation, including dissipation by both thermal conduction and radiation, is numerically solved by making an educated guess for the temperature dependence of the material emissivity, which for Co is not known. The wire emission is recorded as a function of the Joule heat input W into the wire. When melting occurs, the melting temperature fixes the parameter of the emissivity function. The temperature is then computed as a function of the Joule dissipation. Once this is done, we check that the measured wire resistance favorably compares with the one computed by exploiting the known temperature dependence of the Co resistivity and the previously established temperature-power input relationship. As a result, the temperature turns out to be a linear function of the electrical power input

$$T = T_e + \left(\frac{T_M - T_e}{W_M} \right) W \tag{1}$$

in which T_M and W_M are the temperature and electrical power input at melting, respectively, and T_e is the room temperature. We estimate that the uncertainty on T is $\approx \pm 10\,\mathrm{K}$ [30]. A weak, low-frequency ($f \approx 2\,\mathrm{Hz}$) a.c. modulation is superimposed on the d.c. current to slowly modulate the wire temperature so as to allow the use of lock-in (LI) detection techniques.

Two ZnSe lenses image the glowing wire onto a a liquid N_2 cooled photovoltaic HgCdTe detector (Fermionics, mod. PV-12-0.5) of spectral range $0.5\,\mu\mathrm{m} \leq \lambda \lesssim 12\,\mu\mathrm{m}$. The detector output feeds an amplification stage composed by a transimpedance amplifier (Fermionics, PVA-500-10), a linear amplifier (EG&G, PARC, mod. 113), and a LI amplifier (Stanford Research Systems, mod. SR830) and is digitized and recorded by a P.C. for offline analysis. The thermal radiation is analyzed by a ZnSe wire grid, infrared polarizer (Thorlabs, WP25H-Z) mounted on a rotary goniometer. As f is very low, the LI output is averaged for well over 60 s for every position of the goniometer.

The intensity of the emitted radiation is the sum of the unpolarized I_u and of the polarized I_p contributions $I = I_u + I_p$. The analyzer always blocks one half of the polarized component. The voltage output of the lock-in amplifier v_t

is proportional to the radiation intensity impinging on the detector and follows the Malus law $v_t = v_u + v_p \cos^2(\theta - \theta_0)$. $v_u \propto (1/2) I_u$ and $v_p \propto I_p$ are the contributions to the output voltage due to the unpolarized and polarized radiation components, respectively. θ is the polarizer angle and θ_0 is an unessential initial angle. A typical LI output v_t as a function θ is shown in Fig. 1. The average polarization degree is computed as the polarization contrast, defined in any elementary textbooks on Optics, in which the factor of two extinction of the unpolarized light component due to the analyzer has been taken into account

$$P = \frac{I_p}{I_u + I_p} = \frac{v_p}{2v_u + v_p} \tag{2}$$

By using a second analyzer mounted perpendicularly to the first one we ascertained that the polarization is always perpendicular to the wire axis. Thus, by convention, P is taken as positive.

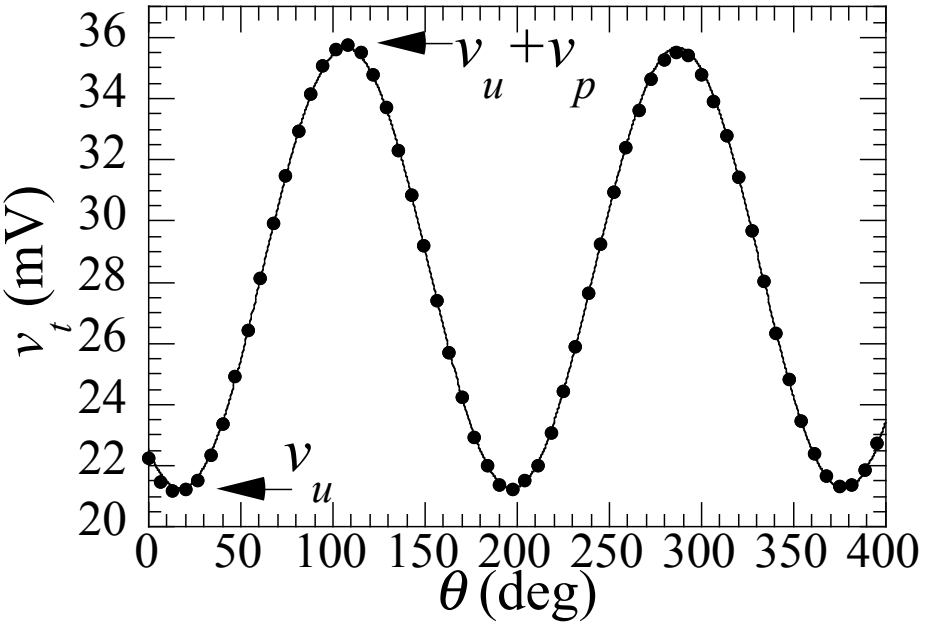

Figure 1: Typical dependence of lock-in output v_t vs. analyzer angle θ. The error bars are of the size of the points. In this figure $P \approx 25.6\,\%$ for a wire at $T \approx 1060\,\mathrm{K}$. The experimental run shown here has an overall time duration of $\approx 3\,\mathrm{hrs}$.

Typically, the current modulation intensity is $\approx 5\,\%$ of the bias current. However, we have checked that P is independent of the current modulation up to a modulation amplitude close to $30\,\%$ of the d.c. bias current.

We would also like to briefly comment on the very different time scales in the experiment that allow use to use LI detection techniques. The Co wire weighs $\approx 5\,\mathrm{mg}$ and its temperature follows any input power change on a time scale extremely shorter than the period of the current modulation. A second time scale is that of the whole apparatus. Once the constant bias current in the wire is changed to reach a different temperature, the apparatus needs at least 0.5 hrs to equilibrate. The polarization measurements are only started once the whole apparatus is in thermal equilibrium as shown by the absence of any long term drift in the data presented in Fig. 1. For this reason, the wire environment is completely decoupled from the rapid changes of the wire temperature occuring in response to the weak and slow (2 Hz) current modulation superimposed to the bias d.c. current that sets the wire temperature.

Finally, as will be described in the next section, there is a much longer time scale in the experiment that is related, in our opinion, to the slow thermally driven dynamics of the wire magnetic structure change.

3. Experimental Results and Discussion

3.1. Phenomenology

We investigated several wires by subjecting them to two different thermal histories. Some wires were kept for a long time each (of the order of 1 week) at high temperature, close to melting, before their temperature was progressively reduced. Wires of a second group, on the contrary, were increasingly heated from room temperature up to melting. Within each group with the same thermal history the repeatability of the results is quite good. For the sake of clarity we only show the typical results obtained for the two different groups. In Fig. 2 P is shown as a function of T for two wires with different thermal histories.

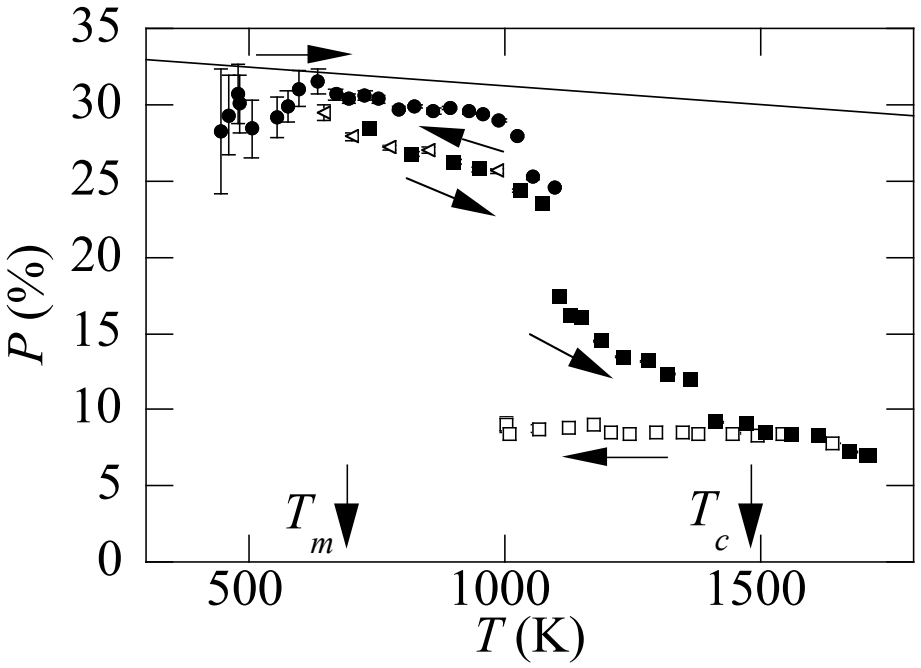

Figure 2: Polarization P vs. temperature T for two cobalt wires with different thermal histories. Line: theoretical expectation for a homogeneous bulk material, Eqn. (3) [26]. Closed circles, open triangles, and closed squares belong to wires heated from room temperature. Closed circles: initial heating process. Open triangles: cooling phase. Closed squares: final heating phase. Open squares: polarization of wires annealed for a long period at high temperature. For these wires the measurements were taken only during cooling. The arrows indicate the thermal path. The error bars are shown on all data points. Except for the lowest T, the point size is comparable with or larger than the experimental error. The martensitic temperature T_m and the Curie temperature T_c are indicated by arrows.

At variance with the tungsten case [30] in which P monotonically decreases with increasing T, the cobalt wires show a hysteretic behavior. The results obtained for wires annealed for a long time at a temperature $T \approx 1600\,\mathrm{K}$ are shown in Fig. 2 as open squares. For these wires, the polarization P of the thermal radiation is rather small ($P \approx 7\,\%$) and remains practically constant upon decreasing T.

On the other hand, wires which have been heated starting from room temperature show a completely different behavior. Upon increasing T in the range $400\,\mathrm{K} \lesssim T \lesssim 1100\,\mathrm{K}$ (closed circles in Fig. 2), P decreases from the theoretically predicted value $P \approx 33\,\%$ down to $P \approx 25\,\%$. Here, the power input is progressively reduced and T is decreased back to $T \approx 650\,\mathrm{K}$ (open triangles). During this backward path the values of P stay smaller than during the heating phase. We believe that this behavior is due to a thermally driven, slow dynamics of the rearrangement of the magnetic domain structure of the wires that will be described next. Finally, the wire teperature is increased again (closed squares) until melting is reached.

For $T \gtrsim 1000\,\mathrm{K}$ P rapidly decreases with increasing T and, eventually, it levels off at the same level of the long annealed wires for high T. We note that the time interval between two successive measurements is $\Delta t \approx 24\,\mathrm{hrs}$.

Additionally, we observe that P behaves smoothly when crossing both the *hcp-fcc* martensitic transition at $T_m \approx 700\,\mathrm{K}$ [33] and the Curie temperature $T_c \approx 1400\,\mathrm{K}$.

3.2. Phenomenological model and results rationalization

The polarization of the thermal radiation emitted by a wire of homogeneous material can be predicted by computing the absorption efficiency factors $Q_{\mathrm{abs}}^{\parallel,\perp}(\lambda, T, R)$ for transverse electrical (TE, $\perp$) and transverse magnetic (TM, $\parallel$) modes of the radiation field impinging on a indefinitely long cylinder of radius R [26, 30, 34, 35] provided that the dependence of the relative dielectric constant ε_r on T and λ is known. For cobalt ε_r is given by a Drude-type form whose parameters are given in literature [36–38]. The observed polarization is given as a function of T and R by

$$P(T,R) = \frac{\langle Q_{\mathrm{abs}}^{\perp}\rangle - \langle Q_{\mathrm{abs}}^{\parallel}\rangle}{\langle Q_{\mathrm{abs}}^{\perp}\rangle + \langle Q_{\mathrm{abs}}^{\parallel}\rangle} \tag{3}$$

in which the average is taken over the accessible wavelength spectrum

$$\langle Q_{\mathrm{abs}}^{\dagger}\rangle = \frac{1}{F}\int \mathcal{D}(\lambda) B(\lambda,T) Q_{\mathrm{abs}}^{\dagger}(\lambda,T,R)\,\mathrm{d}\lambda \quad (\dagger = \perp, \parallel) \tag{4}$$

$B(\lambda, T)$ is the Planck's distribution, $\mathcal{D}(\lambda)$ is the detector responsivity [30], and the normalization is $F = \int \mathcal{D}(\lambda) B(\lambda, T)\, \mathrm{d}\lambda$.

The total radiated intensity can be computed as

$$I = A \left[\langle Q^{\perp}_{\mathrm{abs}} \rangle + \langle Q^{\parallel}_{\mathrm{abs}} \rangle \right] \tag{5}$$

in which A is an unknown constant that takes into account, among others, the solid angle subtended by the source at the detector and must, in principle, be determined by a fit to the experimental results.

The absorption efficiencies for the two modes ($\dagger = \perp, \parallel$) are given by

$$\begin{aligned} Q^{\dagger}_{\mathrm{abs}}(\lambda, T, R) &= \frac{2}{kR} \left[\mathtt{Re} \left(a^{\dagger}_0 + 2 \sum_{m=1}^{\infty} a^{\dagger}_m \right) \right. \\ &\quad \left. + \left(|a^{\dagger}_0|^2 + 2 \sum_{m=1}^{\infty} |a^{\dagger}_m|^2 \right) \right] \end{aligned} \tag{6}$$

with $k = 2\pi/\lambda$. The coefficients $a^{\dagger}_m$ are obtained by enforcing the suitable boundary conditions, thereby yielding

$$a^{\perp}_m = \frac{J'_m(nkR) J_m(kR) - n J_m(nkR) J'_m(kR)}{J'_m(nkR) H^{(2)}_m(kR) - n J_m(nkR) H^{(2)\prime}_m(kR)} \tag{7}$$

$$a^{\parallel}_m = \frac{n J'_m(nkR) J_m(kR) - J_m(nkR) J'_m(kR)}{n J'_m(nkR) H^{(2)}_m(kR) - J_m(nkR) H^{(2)\prime}_m(kR)} \tag{8}$$

in which $n = \sqrt{\varepsilon_r}$ is the complex refraction index, J_m and $H^{(2)}_m$ are the Bessel functions of first kind and the Hankel functions of second kind, respectively. The solid line in Fig. 2 is the prediction of Eqn. (3) for a wire of nominal radius $R_0 = 50\,\mu$m. Evidently, the prediction of P for a homogeneous material completely disagrees with the experimental data, except at the lowest T where $P \approx 30\,\%$ is a universal limit for $\lambda_T \geq R$, independent of the material [26]. For any other T, P is lower than predicted.

However, the polarization P computed according to Eqn. (3) strongly depends on R at any T as shown in Fig. 3. As R decreases, P decreases as well, and, for very small R, it also becomes negative, i.e., parallel to the wire axis. Upon decreasing R the phase space available to the transverse modes of collective charge fluctuations is shrinked and P gets smaller than in larger wires. For

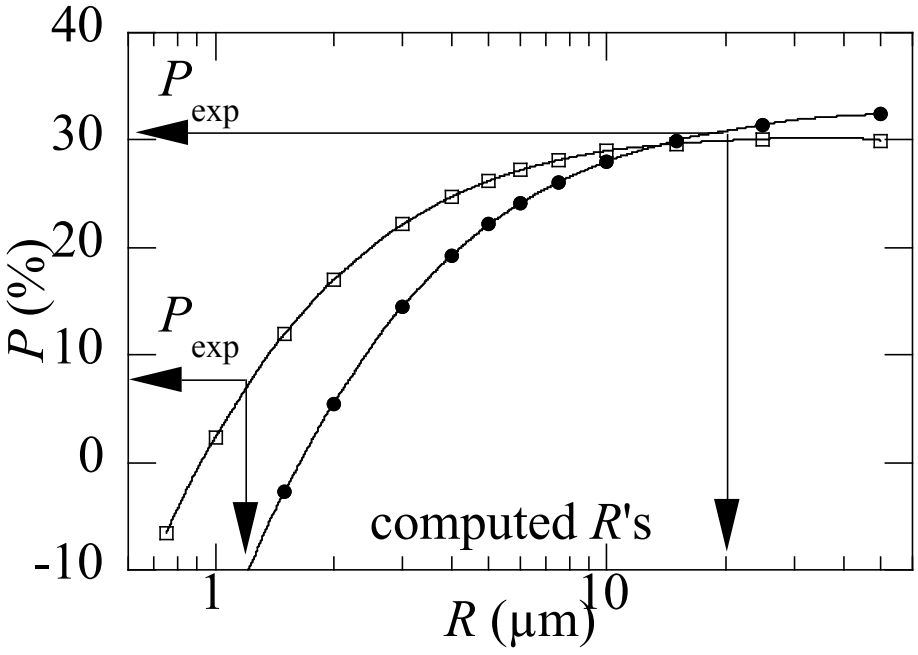

Figure 3: Polarization degree P vs. wire radius R computed for $T = 500\,\mathrm{K}$ (closed points) and for $T = 1500\,\mathrm{K}$ (open squares). $P > 0$ indicates that the polarization is perpendicular to the wire axis, whereas for $P < 0$ the polarization has rotated parallel to the wire axis. The lines are an eyeguide only.

very thin wires the polarization direction can even rotate by $\pi/2$ and become parallel to the wire axis, yielding $P < 0$. We remind that in our experiment P always remains perpendicular to the wire, i.e., $P > 0$.

At the same time, the computation shows that the intensity radiated per unit wire surface j is practically independent of R and the total radiated intensity $I \propto 2v_u + v_p$, which is the other experimentally measured quantity, is proportional to R, $I = jR$. As a consequence, a bundle of $N = R_0/R$ wires of radius $R < R_0$ would radiate the same intensity I as the larger wire of radius R_0 but P would turn out be smaller.

This observation suggests that the thermally induced demagnetization of the cobalt wire might explain the observed behavior of P as a function of T. Let us consider the following very crude model depicted in Fig. 4.

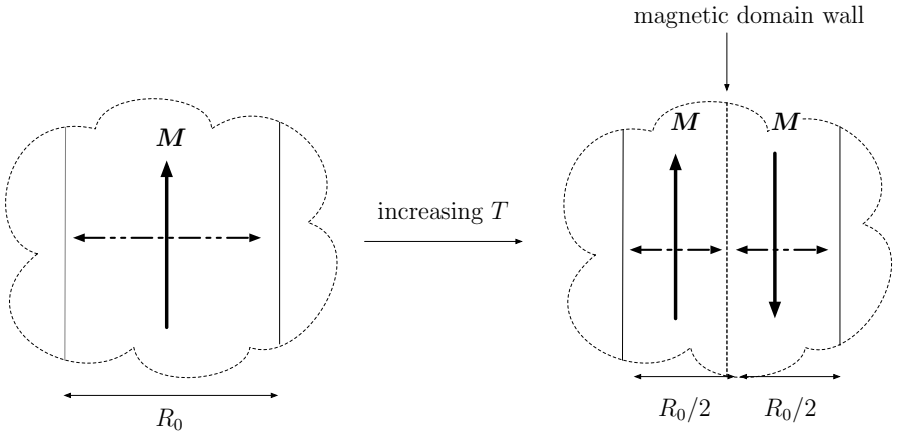

Figure 4: Crude model to rationalize the decrease of P with increasing T due to thermally induced wire demagnetization. M: remanent magnetization. Dash-dotted lines: range available for transverse modes of collective charge fluctuations.

Let us assume that the wire at room temperature consists of a dominant magnetic domain with the magnetization aligned parallel to the wire long axis because of magnetoelastic anisotropy resulting from the coupling between the internal stresses due to the drawing production process and magnetostriction. Clearly, the fine structure of the magnetic domains depends on several factors including, among many others, geometry, magnetic history, and mechanical stresses of the material [39]. Nonetheless, we believe that the present simplified model is adequate for our purposes.

The transverse modes of charge fluctuations can span the whole wire diameter (left part of Fig. 4). Upon increasing T, thermally driven DW motion takes places and a domain with reversed magnetization grows larger in order to reduce the magnetic energy (right part of Fig. 4). As the typical thickness of the DW is much larger than the typical electron wavelength at the Fermi level [40], the DW offers a enhanced resistance [41–49] across the wire. This impedance mismatch at the DW would produce reflection of the collective charge fluctuations transverse modes thereby shrinking their available spatial range and lowering the long wavelength cutoff. In such a way P is reduced but the radiated intensity would

remain the same. By increasing T, this process keeps occurring, thereby leading to a further subdivision of the wire in gradually thinner magnetic domains.

We believe that the DW motion is thermally driven diffusion [7] for several reasons. Current-driven DW motion is ruled out because it requires current densities at least in excess of $\approx 10^9 - 10^{10}\,\mathrm{A/m^2}$ [3, 50] whereas in our experiment the maximum current density is $\lesssim 1.8 \times 10^8\,\mathrm{A/m^2}$. Moreover, in the present case the current is flowing parallel rather than perpendicular to the DW's. Magnetic field-driven DW motion is also ruled out because the wire is mounted in a magnetic material free environment. The only magnetic field in the experiment is generated by the current itself flowing in the wire, lies in planes perpendicular to the wire axis, and does not exceed the value $H \approx 4\,\mathrm{kA/m}$ at the wire circumference for the highest current used in the experiment. Moreover, as the typical time scale for a polarization change to occur in our experiment is $\tau \sim 10^5\,\mathrm{s}$, the estimate of the strength E of activation energy barriers for thermal activation of magnetization reversal would yield $E/k_\mathrm{B}T > 35$ [12], a value which seems quite too large. Additionally, we note that diffusive DW motion may show a hysteretic behavior [1] as observed in our experiment.

According to the present model, we can estimate the radius $R(T)$ of the wires in the bundle by solving for R the equation $P(T, R(T)) = P_\mathrm{exp}$, where P_exp is the measured polarization value, as shown in Fig. 3. The resulting R is shown as a function of T in Fig. 5. Within the conceptual framework of this model, R can be thought of as an estimate of the average transverse size of the magnetic domains. Upon increasing T from room temperature, R decreases from the nominal value of $50\,\mu\mathrm{m}$ down to $\approx 10\,\mu\mathrm{m}$. After the polarization drop for $T \approx 1100\,\mathrm{K}$, during the cooling phase, R shows hysteresis by remaining smaller than during the initial heating. Upon the final reheating, R steadily decreases and reaches the value $R \approx 1\,\mu\mathrm{m}$ just before melting. This behavior is coherent with a thermally induced demagnetization process of the sample as detected in several different types of measurements [16, 17, 20, 51].

Additionally, it is interesting to note that at high temperatures around and above the Curie temperature T_c the polarization of the thermal radiation emit-

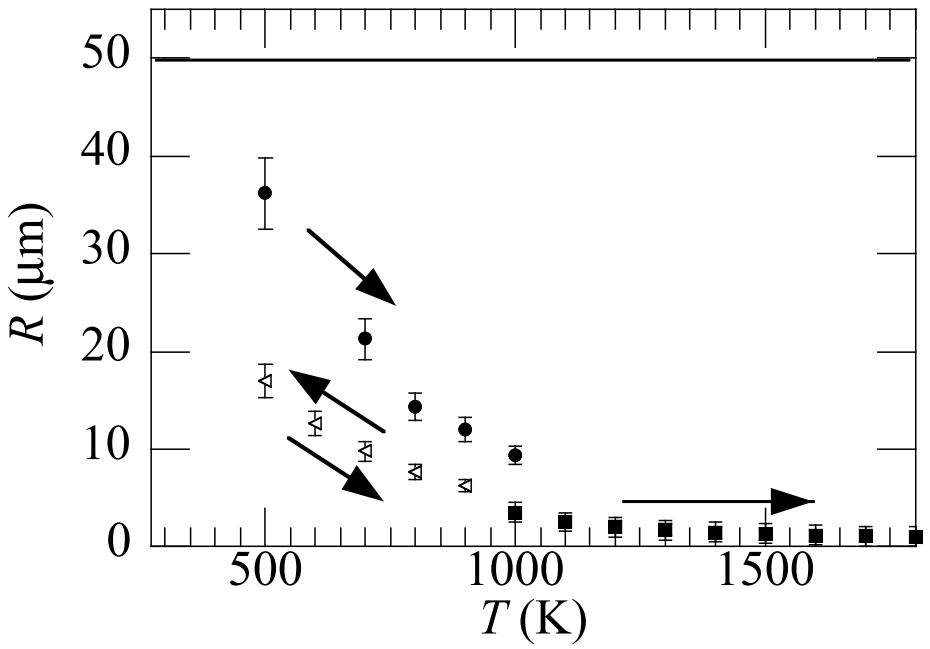

Figure 5: Radius of the wires in the bundle $R(P)$ computed from the measured P vs. T. Solid line: nominal wire radius. Closed circles: initial heating. Triangles: cooling and reheating. Closed squares: final heating. Arrows: thermal path direction.

ted by wires with different thermal history becomes equal. According to the Weiss' view, the paramagnetic phase consists of a large number of small, randomly oriented magnetic domains whose boundaries still limit the range of the collective fluctuations of the electron gas. This, in our opinion, might be the rationale of the observed low value of the polarization degree at high temperature.

At the same time, according to our expectations, the total radiated intensity I should be insensitive to the bundle structure and should only depend on T. Actually, this is the case, as shown in Fig. 6, where the measured I is compared with the theoretical prediction $I \propto \langle Q^{\perp}_{\rm abs}\rangle + \langle Q^{\parallel}_{\rm abs}\rangle$ evaluated at the temperature dependent radius R shown in Fig. 5. The agreement between experiment and theory is relatively satisfactory.

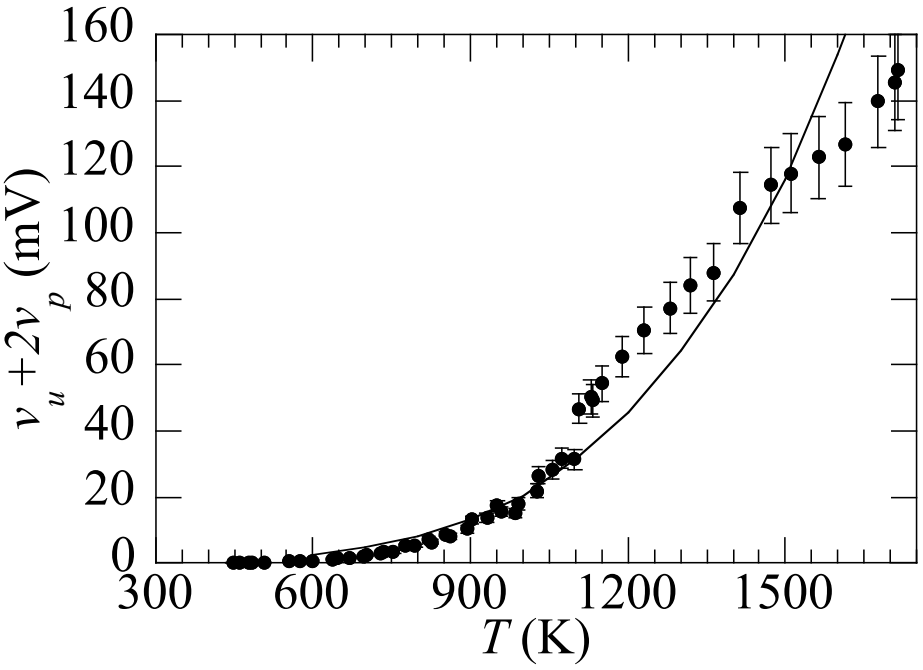

Figure 6: Total LI output $v_u + 2v_p$ vs. temperature T. Closed point: experiment. Solid line: computed total radiated intensity I. The normalization factor A in Eqn. (5) is chosen so as to minimize the deviations from the experimental points.

4. Conclusions

We have presented in this paper the experimental measurements of the polarization degree of the thermal radiation emitted by thin Co wires. An unexpected behavior, compared to the polarization trend measured in tungsten wires, has been observed and reported here for the first time. Moreover, we have suggested a possible explanation of the experimental outcome to be traced back to a progressive, thermally driven sample demagnetization leading to a decrease of the transverse size of the magnetic domains as the wire temperature is increased.

We are well aware that the crude model we have devised is very speculative and is only supported by indirect observations. However, we emphasize the fact that no experiments of this kind with a magnetic material have ever been carried out.

As a conclusion we can thus state that optical measurements on macroscopic magnetic materials can shed light on the temperature evolution of the magnetic domain structure of the material itself. Actually, the piece of information that this kind of measurements can provide is only macroscopic and, in some sense, of thermodynamic nature because it does not give any insight into the microscopic structure of the sample. At the same time, we would like to emphasize that the present results are quite satisfactory even taking into account the extreme sensitivity of the magnetic material properties to, among others, composition, manufacturing, annealing, and ageing of the sample.

Future development based on the study of the polarization of the thermal radiation emitted by ferromagnetic and paramagnetic samples could take advantage of the presence of a strong, orientable and static magnetic field driving the domain nucleation. These studies, in addition to the opportunity to test the crude model presented in this manuscript, could furthermore lead to the use of this method for investigating the bulk properties of micro- and nano-specimens.

Acknowledgments

We thank dr. P. G. Antonini, G. Galet, and E. Berto for technical assistance.

References

[1] T. Nattermann, V. Pokrovsky, V. M. Vinokur, Hysteretic Dynamics of Domain Walls at Finite Temperatures, Phys. Rev. Lett. 87 (2001) 197005. doi:10.1103/PhysRevLett.87.197005.

[2] P. J. Metaxas, J. P. Jamet, A. Mougin, M. Cormier, J. Ferré, V. Baltz, B. Rodmacq, B. Dieny, R. L. Stamps, Creep and Flow Regimes of Magnetic Domain-Wall Motion in Ultrathin Pt/Co/Pt Films with Perpendicular Anisotropy, Phys. Rev. Lett. 99 (2007) 217208. doi:10.1103/PhysRevLett.99.217208.

[3] S. DuttaGupta, S. Fukami, B. Kuerbanjiang, H. Sato, F. Matsukura, V. K. Lazarov, H. Ohno, Magnetic domain-wall creep driven by field and current in Ta/CoFeB/MgO, AIP Advances 7 (5) (2017) 055918. doi:10.1063/1.4974889.

[4] S. Zapperi, P. Cizeau, G. Durin, H. E. Stanley, Dynamics of a ferromagnetic domain wall: Avalanches, depinning transition, and the Barkhausen effect, Phys. Rev. B 58 (1998) 6353–6366. doi:10.1103/PhysRevB.58.6353.

[5] P. Chauve, T. Giamarchi, P. Le Doussal, Creep and depinning in disordered media, Phys. Rev. B 62 (2000) 6241–6267. doi:10.1103/PhysRevB.62.6241.

[6] M. Hayashi, L. Thomas, C. Rettner, R. Moriya, S. S. P. Parkin, Direct observation of the coherent precession of magnetic domain walls propagating along permalloy nanowires, Nature Phys. 3 (2007) 21–25. doi:10.1038/nphys464.

[7] J. Leliaert, B. Van de Wiele, J. Vandermeulen, A. Coene, A. Vansteenkiste, L. Laurson, G. Durin, B. Van Waeyenberge, L. Dupré, Thermal effects on transverse domain wall dynamics in magnetic nanowires, Applied Physics Letters 106 (2015) 202401. doi:10.1063/1.4921421.

[8] K. Ounadjela, R. Ferré, L. Louail, J. M. George, J. L. Maurice, L. Piraux, S. Dubois, Magnetization reversal in cobalt and nickel electrodeposited nanowires, Journal of Applied Physics 81 (1997) 5455–5457. doi:10.1063/1.364568.

[9] M. Brands, R. Wieser, C. Hassel, D. Hinzke, G. Dumpich, Reversal processes and domain wall pinning in polycrystalline Co-nanowires, Phys. Rev. B 74 (2006) 174411. doi:10.1103/PhysRevB.74.174411.

[10] A. I. Dmitriev, A. D. Talantsev, E. I. Kunitsyna, R. B. Morgunov, V. P. Piskorskii, O. G. Ospennikova, E. N. Kablov, Magnetic noise

as the cause of the spontaneous magnetization reversal of RE–TM–B permanent magnets, J. Exp. Theor. Phys. 123 (2016) 303–307. doi:10.1134/S106377611606011X.

[11] P. Gaunt, The frequency constant for thermal activitation of a ferromagnetic domain wall, J. Appl. Phys. 48 (1977) 3470–3474. doi:10.1063/1.324195.

[12] P. Gaunt, Magnetic viscosity and thermal activation energy, J. Appl. Phys. 59 (1986) 4129–4132. doi:10.1063/1.336671.

[13] V. K. Joshi, Spintronics: A contemporary review of emerging electronics devices, Eng. Sci. Technol. 19 (2016) 1503 – 1513. doi:10.1016/j.jestch.2016.05.002.

[14] S. S. S. P. Parkin, M. Hayashi, L. Thomas, Magnetic Domain-Wall Racetrack Memory, Science 320 (2008) 190–194. doi:10.1126/science.1145799.

[15] M. Diegel, R. Mattheis, E. Halder, 360/spl deg/ domain wall investigation for sensor applications, IEEE Trans. Magn. 40 (2004) 2655–2657. doi:10.1109/TMAG.2004.830434.

[16] H. U. Worm, M. Jackson, P. Kelso, S. K. Banerjee, Thermal demagnetization of partial thermoremanent magnetization, J. Geophys. Res. 93 (1988) 12196–12204. doi:10.1029/JB093iB10p12196.

[17] F. Heider, S. L. Halgedahl, D. J. Dunlop, Temperature dependence of magnetic domains in magnetite crystals, Geophys. Res. Lett. 15 (1988) 499–502. doi:10.1029/GL015i005p00499.

[18] C. A. Fowler, E. M. Fryer, Magnetic Domains by the Longitudinal Kerr Effect, Phys. Rev. 94 (1954) 52–56. doi:10.1103/PhysRev.94.52.

[19] D. Weller, G. R. Harp, R. F. C. Farrow, A. Cebollada, J. Sticht, Orientation dependence of the polar Kerr effect in fcc and hcp Co, Phys. Rev. Lett. 72 (1994) 2097–2100. doi:10.1103/PhysRevLett.72.2097.

[20] K. Ono, J. Fujii, A. Kakizaki, T. Ikoma, T. Kinoshita, T. Ishii, K. Tanaka, K. Shimada, Y. Saitoh, T. Sendohda, H. Fukutani, Temperature dependence of magneto-optic Kerr effect and spin-resolved photoemission of Ni(110), J. Magn. Magn. Mat. 148 (1995) 74 – 75. doi:https://doi.org/10.1016/0304-8853(95)00155-7.

[21] A. Chizhik, A. Zhukov, J. Blanco, J. Gonzalez, Magneto-optical investigation of the magnetization reversal in co-rich wires, Physica B: Condensed Matter 299 (2001) 314–321. doi:10.1016/S0921-4526(01)00483-5.

[22] A. Chizhik, J. Gonzalez, A. Zhukov, J. M. Blanco, Magnetization reversal of co-rich wires in circular magnetic field, Journal of Applied Physics 91 (1) (2002) 537–539. arXiv:https://aip.scitation.org/doi/pdf/10.1063/1.1421209, doi:10.1063/1.1421209.
URL https://aip.scitation.org/doi/abs/10.1063/1.1421209

[23] A. Chizhik, J. Gonzalez, J. Yamasaki, A. Zhukov, J. M. Blanco, Vortex-type domain structure in Co-rich amorphous wires, Journal of Applied Physics 95 (2004) 2933–2935. doi:10.1063/1.1646439.

[24] A. Chizhik, V. Zablotskii, A. Stupakiewicz, C. Gómez-Polo, A. Maziewski, A. Zhukov, J. Gonzalez, J. M. Blanco, Magnetization switching in ferromagnetic microwires, Phys. Rev. B 82 (2010) 212401. doi:10.1103/PhysRevB.82.212401.

[25] C. Galea, M. Shneider, A. Dogariu, R. Miles, Magnetically Induced Depolarization of Microwave Scattering from a Laser-Generated Plasma, Phys. Rev. Applied 12 (2019) 034055. doi:10.1103/PhysRevApplied.12.034055.

[26] B. Agdur, G. Böling, F. Sellberg, Y. Öhman, Scattering, Absorption, and Emission of Light by Thin Metal Wires, Phys. Rev. 130 (1963) 996–1001. doi:10.1103/PhysRev.130.996.

[27] S. Ingvarsson, L. J. Klein, Y.-Y. Au, J. A. Lacey, H. F. Hamann, Enhanced thermal emission from individual antenna-like nanoheaters, Opt. Express 15 (2007) 11249–11254. doi:10.1364/OE.15.011249.

[28] Y.-Y. Au, H. S. Skulason, S. Ingvarsson, L. J. Klein, H. F. Hamann, Thermal radiation spectra of individual subwavelength microheaters, Phys. Rev. B 78 (2008) 085402. doi:10.1103/PhysRevB.78.085402.

[29] L. J. Klein, S. Ingvarsson, H. F. Hamann, Changing the emission of polarized thermal radiation from metallic nanoheaters, Opt. Express 17 (2009) 17963–17969. doi:10.1364/OE.17.017963.

[30] A. F. Borghesani, G. Carugno, Temperature dependent polarization of the thermal radiation emitted by thin, hot tungsten wires, Int. J. Therm. Sci. 104 (2016) 101 – 111. doi:10.1016/j.ijthermalsci.2015.12.020.

[31] T. Nishizawa, K. Ishida, The Co (Cobalt) system, Bull. Alloy Phase Diag. 4 (1983) 387–390. doi:10.1007/BF02868089.

[32] D. Richardson, S. Katz, J. Wang, Y. K. Takahashi, K. Srinivasan, A. Kalitsov, K. Hono, A. Ajan, M. Wu, Near-Tc Ferromagnetic Resonance and Damping in FePt-Based Heat-Assisted Magnetic Recording Media, Phys. Rev. Applied 10 (2018) 054046. doi:10.1103/PhysRevApplied.10.054046.

[33] P. Tolédano, G. Krexner, M. Prem, H.-P. Weber, V. P. Dmitriev, Theory of the martensitic transformation in cobalt, Phys. Rev. B 64 (2001) 144104. doi:10.1103/PhysRevB.64.144104.

[34] G. Bimonte, L. Cappellin, G. Carugno, G. Ruoso, D. Saadeh, Polarized thermal emission by thin metal wires, New Journal of Physics 11 (2009) 033014. doi:10.1088/1367-2630/11/3/033014.

[35] V. A. Golyk, M. Krüger, M. Kardar, Heat radiation from long cylindrical objects, Phys. Rev. E 85 (2012) 046603. doi:10.1103/PhysRevE.85.046603.

[36] T. Makino, H. Kawasaki, T. Kunitomo, Study of the Radiative Properties of Heat Resisting Metals and Alloys : (1st Report, Optical Constants and Emissivities of Nickel, Cobalt and Chromium), Bulletin of JSME 25 (1982) 804–811. doi:10.1299/jsme1958.25.804.

[37] M. A. Ordal, L. L. Long, R. J. Bell, S. E. Bell, R. R. Bell, R. W. Alexander, C. A. Ward, Optical properties of the metals Al, Co, Cu, Au, Fe, Pb, Ni, Pd, Pt, Ag, Ti, and W in the infrared and far infrared, Appl. Opt. 22 (1983) 1099–1119. doi:10.1364/AO.22.001099.

[38] M. A. Ordal, R. J. Bell, R. W. Alexander, L. L. Long, M. R. Querry, Optical properties of fourteen metals in the infrared and far infrared: Al, Co, Cu, Au, Fe, Pb, Mo, Ni, Pd, Pt, Ag, Ti, V, and W., Appl. Opt. 24 (1985) 4493–4499. doi:10.1364/AO.24.004493.

[39] F. Lofink, A. Philippi-Kobs, M. R. Rahbar Azad, S. Hankemeier, G. Hoffmann, R. Frömter, H. P. Oepen, Domain Walls in Bent Nanowires, Phys. Rev. Applied 8 (2017) 024008. doi:10.1103/PhysRevApplied.8.024008.

[40] G. Tatara, H. Kohno, J. Shibata, Microscopic approach to current-driven domain wall dynamics, Phys. Rep. 468 (2008) 213–301. doi:10.1016/j.physrep.2008.07.003.

[41] G. G. Cabrera, L. M. Falicov, Theory of the Residual Resistivity of Bloch Walls I. Paramagnetic Effects, Phys. Status Solidi B 61 (1974) 539–549. doi:10.1002/pssb.2220610219.

[42] G. G. Cabrera, L. M. Falicov, Theory of the Residual Resistivity of Bloch Walls. II. Inclusion of Diamagnetic Effects, Phys. Status Solidi B 62 (1974) 217–222. doi:10.1002/pssb.2220620122.

[43] C. Dupas, P. Beauvillain, C. Chappert, J. P. Renard, F. Trigui, P. Veillet, E. Vélu, D. Renard, Very large magnetoresistance effects induced by antiparallel magnetization in two ultrathin cobalt films, J. Appl. Phys. 67 (1990) 5680–5682. doi:10.1063/1.345925.

[44] P. M. Levy, S. Zhang, Resistivity due to domain wall scattering, Phys. Rev. Lett. 79 (1997) 5110–5113. doi:10.1103/PhysRevLett.79.5110.

[45] U. Rüdiger, J. Yu, L. Thomas, S. S. P. Parkin, A. D. Kent, Magnetoresistance, micromagnetism, and domain-wall scattering in epitaxial hcp co films, Phys. Rev. B 59 (1999) 11914–11918. doi:10.1103/PhysRevB.59.11914.

[46] U. Ebels, A. Radulescu, Y. Henry, L. Piraux, K. Ounadjela, Spin Accumulation and Domain Wall Magnetoresistance in 35 nm Co Wires, Phys. Rev. Lett. 84 (2000) 983–986. doi:10.1103/PhysRevLett.84.983.

[47] A. D. Kent, J. Yu, U. Rüdiger, S. S. P. Parkin, Domain wall resistivity in epitaxial thin film microstructures, J. Phys.: Condensed Matter 13 (2001) R461–R488. doi:10.1088/0953-8984/13/25/202.

[48] B. Leven, G. Dumpich, Resistance behavior and magnetization reversal analysis of individual Co nanowires, Phys. Rev. B 71 (2005) 064411. doi:10.1103/PhysRevB.71.064411.

[49] W. Boonruesi, J. Chureemart, P. Chureemart, Calculation of domain wall resistance in magnetic nanowire, Appl. Phys. Lett. 115 (7) (2019) 072408. doi:10.1063/1.5101006.

[50] R. Díaz Pardo, N. Moisan, L. J. Albornoz, A. Lemaître, J. Curiale, V. Jeudy, Common universal behavior of magnetic domain walls driven by spin-polarized electrical current and magnetic field, Phys. Rev. B 100 (2019) 184420. doi:10.1103/PhysRevB.100.184420.

[51] W. Szmaja, K. Polański, K. Dolecki, The temperature dependence of magnetic domain structure in cobalt monocrystals studied by SEM, J. Magn. Magn. Mat. 151 (1995) 249–258. doi:10.1016/0304-8853(95)00327-4.